TBSD#1871415, VOL 0, ISS 0

ACE2-derived peptides interact with the RBD domain of SARS-CoV-2 spike glycoprotein, disrupting the interaction with the human ACE2 receptor

Pedro F. N. Souza, Jackson L. Amaral, Leandro P. Bezerra, Francisco E. S. Lopes, Valder N. Freire, Jose T. A. Oliveira, and Cleverson D. T. Freitas

QUERY SHEET

This page lists questions we have about your paper. The numbers displayed at left are hyperlinked to the location of the query in your paper.

The title and author names are listed on this sheet as they will be published, both on your paper and on the Table of Contents. Please review and ensure the information is correct and advise us if any changes need to be made. In addition, please review your paper as a whole for typographical and essential corrections.

Your PDF proof has been enabled so that you can comment on the proof directly using Adobe Acrobat. For further information on marking corrections using Acrobat, please visit http://journalauthors.tandf.co.uk/production/acrobat.asp; https://authorservices.taylorandfrancis.com/how-to-correct-proofs-with-adobe/

The CrossRef database (www.crossref.org/) has been used to validate the references.

AUTHOR QUERIES

Q1 Please check and confirm the edits made in affiliation "c" and correspondence.

Q2 Please check the sentence "For example, Qiao and Olvera de la Cruz (2020) reported … " for clarity.

Q3 Please check the edits made in the sentence “The minimization was performed … ”.

Q4 Please check the edit made in "Funding" heading. Also check that author statement has been deleted as it is not mentioned in stylesheet.

Q5 There is no mention of [Hall & Ji (2020), Henderson et al. (2020), Ngo et al. (2020), Othman et al. (2020)] in the text. Please insert a citation in the text or delete the reference as appropriate, maintaining the numerical order of the references

Q6 Please provide editor names and publisher name.

Q7 Please provide the volume number.

Q8 Please provide the volume number and page range.

Q9 Please provide editor names for "Peiris (2012)".

Q10 Please note that the ORCID section has been created from information supplied with your manuscript submission/CATS. Please correct if this is inaccurate.

JOURNAL OF BIOMOLECULAR STRUCTURE AND DYNAMICS
https://doi.org/10.1080/07391102.2020.1871415

ACE2-derived peptides interact with the RBD domain of SARS-CoV-2 spike glycoprotein, disrupting the interaction with the human ACE2 receptor

Q10 Pedro F. N. Souza[a], Jackson L. Amaral[a,b], Leandro P. Bezerra[a], Francisco E. S. Lopes[c], Valder N. Freire[b], Jose T. A. Oliveira[a] and Cleverson D. T. Freitas[a]

[a]Department of Biochemistry and Molecular Biology, Federal University of Ceará, Fortaleza, Brazil;; [b]Department of Physics, Federal University of Ceará, Fortaleza, Brazil; [c]Center for Permanent Education in Health Care, CEATS/School of Public Health of Ceará-ESP-CE, Universidade Federal do Ceará, Fortaleza, Brazil

Communicated by Ramaswamy H. Sarma

ABSTRACT

Vaccines could be the solution to the current SARS-CoV-2 outbreak. However, some studies have shown that the immunological memory only lasts three months. Thus, it is imperative to develop pharmacological treatments to cope with COVID-19. Here, the *in silico* approach by molecular docking, dynamic simulations and quantum biochemistry revealed that ACE2-derived peptides strongly interact with the SARS-CoV-2 RBD domain of spike glycoprotein (S-RBD). ACE2-Dev-PepI, ACE2-Dev-PepII, ACE2-Dev-PepIII and ACE2-Dev-PepIV complexed with S-RBD provoked alterations in the 3D structure of S-RBD, leading to disruption of the correct interaction with the ACE2 receptor, a pivotal step for SARS-CoV-2 infection. This wrong interaction between S-RBD and ACE2 could inhibit the entry of SARS-CoV-2 in cells, and thus virus replication and the establishment of COVID-19 disease. Therefore, we suggest that ACE2-derived peptides can interfere with recognition of ACE2 in human cells by SARS-CoV-2 *in vivo*. Bioinformatic prediction showed that these peptides have no toxicity or allergenic potential. By using ACE2-derived peptides against SARS-CoV-2, this study points to opportunities for further *in vivo* research on these peptides, seeking to discover new drugs and entirely new perspectives to treat COVID-19.

ARTICLE HISTORY
Received 13 October 2020
Accepted 29 December 2020

KEYWORDS
SARS-CoV-2 RBD; COVID-19; ACE2 receptor; ACE2-derived peptides

1. Introduction

Coronaviruses (CoVs) are enveloped and pleomorphic viruses belonging to the Coronaviridae family. They share a typical morphology with the non-segmented positive single-stranded RNA genome, estimated to have length of 30 Kb (Burrell et al., 2017; Peiris, 2012). The human-to-human spread of the coronaviruses is mainly by nose and mouth secretion droplets. These viruses cause disease that ranges from mild cold symptoms to atypically severe pneumonia, with many complications, resulting in death (Burrell et al., 2017).

The current pandemic caused by the severe acute respiratory syndrome coronavirus 2 (SARS-CoV-2) has claimed many lives and threatened thousands worldwide. Coronavirus disease 2019 (COVID-19) is less lethal and by far more transmissible than the diseases caused by the viruses involved in other recent outbreaks, such as in 2002 by severe acute respiratory syndrome coronavirus (SARS-CoV) and Middle East respiratory syndrome coronavirus (MERS-CoV). A way to measure that is the case fatality rate (CRF) of each outbreak. The CRF of SARS-CoV, MERS-CoV and SARS-CoV-2 is, respectively, of 9.7, 34 and 1%, which indicates that SARS-CoV-2 is not one of the worst coronaviruses. However, its higher transmissibility has resulted in 10 million of infected people with 500 000 deaths, by far a larger number compared to other outbreaks (Andersen et al., 2020; Li et al., 2020; Song et al., 2019).

SARS-CoV-2 is close to SARS-CoV-1, sharing similarities accounting nearly 80% in the genome sequence. Additionally, both coronaviruses employ the same receptor-binding domain (RBD) in the spike glycoprotein (S protein) to interact with human angiotensin-converting enzyme 2 (ACE2) of the host cell to start the infection. The virus takes control of the cellular machinery to synthesize its own genome and proteins. Despite similarities, the SARS-CoV-2 S protein has accumulated mutations, leading to modifications in the RBD region that enhance its affinity for human ACE2 20-fold compared to SARS-CoV S protein, resulting in faster transmission from human to human (Andersen et al., 2020; Walls et al., 2020; Yuan et al., 2017).

Despite the similarities, it is important to highlight the differences between SARS-CoV-1 and SARS-CoV-2 receptor recognition as they are involved in virus transmissibility, infectivity and pathology. It is known that the SARS-CoV-2 RBD has a higher ACE2-binding affinity than SARS-CoV-1, a characteristic which could lead to a more efficient cell entry and transmissibility (Walls et al., 2020; Yan et al., 2020). In

CONTACT Pedro F. N. Souza pedrofilhobio@gmail.com Laboratory of Plant Defense Proteins, Biochemistry and Molecular Biology Department, Federal University of Ceará, Av. Mister Hull, Fortaleza, CE 60451, Brazil

Supplemental data for this article can be accessed online at https://doi.org/10.1080/07391102.2020.1871415.

contrast, ACE2 affinity toward the entire SARS-CoV-2 S protein is lower than that of SARS-CoV entire S protein suggesting that SARS-CoV-2 RBD, besides being strongest, is probably less exposed than SARS-CoV RBD (Andersen et al., 2020; Song et al., 2019; Walls et al., 2020; Yan et al., 2020; Yuan et al., 2017). In addition, SARS-CoV-2 S protein also held substitution D614G during the coronavirus disease 2019 (COVID-19) pandemic (Sheffield COVID-19 Genomics Group, 2020). An elegant experiment using the cryoelectron microscopy (cryo-EM) revealed that the change from D614 to G614 eliminates the requirements of side-chain hydrogen bond, increasing mainchain flexibility and altering interactions, and modulates glycosylation enhancing the cell entry, infectivity, transmissibility, stability of virions and high viral loads in the airways (Sheffield COVID-19 Genomics Group, 2020; Wrapp et al., 2020). Besides these differences, a new feature is the high nanomechanical stability of the SARS-CoV-2 S-ACE2 interaction compared to SARS-CoV-1 (Moreira et al., 2020). Moreira et al. (2020) revealed that high mechanical stability in the SARS-CoV-2 S-ACE2 has several biological implications such as cell recognition, viral attachment, fusion and entry. Thus, mechanical stability might play a role in the increasing spread of COVID-19 (Moreira et al., 2020).

Still regarding the importance of S-ACE2 interaction for SARS-CoV-2 cell entry, there recently have been reported that mutations far from RBD could affect the S-ACE2 interaction (Qiao & Olvera de la Cruz, 2020). For example, Qiao and Olvera de la Cruz (2020) reported mutations non-RBD sited, but altering the polybasic cleavage could result in 34% of the S-RBD strength of interaction. This result suggests the role of polybasic cleavage in enhancement of S-ACE2 interaction (Qiao & Olvera de la Cruz, 2020).

Given the importance of the S-ACE2 interaction to COVID-19 establishment, many studies have focused on finding drugs (either already available or new ones) that can interfere with this interaction, making S protein a promising target in *silico* assays. Other groups have been investigating existing drugs used to treat other viral infections, in a process called repositioning or repurposing, but without success (Calligari et al., 2020). Nevertheless, computational screening is an exciting approach to develop new drugs faster and more precisely. Therefore, many research groups are employing molecular docking (MD) and molecular dynamic simulation (MDS) to find new molecules targeting the SARS-CoV-2 S protein (Calligari et al., 2020; Souza et al., 2020).

Recently, our research group performed MD and MDS studies using eight synthetic antimicrobial peptides (*Mo*-CBP3-PepI, *Mo*-CBP3-PepII, *Mo*-CBP3-PepIII, *RcAlb*-PepI, *RcAlb*-PepII, *RcAlb*-PepIII, PEPGAT and PEPKAA) to target the SARS-CoV-2 S glycoprotein (Souza et al., 2020). Of those, *Mo*-CBP3-PepII and PEPKAA strongly interacted with the SARS-COV-2 S protein, changing its native conformation and topology, leading to wrong interaction with ACE2 (Souza et al., 2020).

The most crucial feature of the SARS-CoV-2 S protein is the high affinity of the RBD domain to the human ACE2 receptor, leading to higher levels of infection compared to SARS-CoV and MERS-CoV. Based on that, in this study, we employed the sequence to design antiviral peptides targeting the SARS-CoV-2 S protein RBD domain (S-RBD). Altogether, molecular docking, dynamic simulations and quantum biochemical analyses revealed that all peptides strongly bind to the RBD domain of SARS-CoV-2 S protein. Through this binding, the peptides can stop the correct cross talk between the cell and SARS-CoV-2, which is a critical step in the viral infection. Therefore, the inhibition or induction of incorrect interaction of the RBD domain and the human ACE2 receptor could be a potentially valuable strategy to combat COVID-19 caused by SARS-CoV-2.

2. Methodology

2.1. Design of peptides

The design of peptides followed the pipeline produced by Souza et al. (2020). The protein sequence chosen was angiotensin-converting enzyme 2 from *Homo sapiens* (ACE2), freely available in the NCBI database (https://www.ncbi.nlm.nih.gov/) under accession number Q9BYF1. The server used for the design was the AVPpred server (http://crdd.osdd.net/servers/avppred/) according to Thakur et al. (2012). First, the sequence of ACE2 was fractioned using AVPpred to produce peptides with chain lengths of 10, 15 and 20 amino acid residues. Then, all the peptides were run in AVPpred to find potential antiviral peptides. The AVPpred algorithm employs three criteria to select peptides: (1) alignment model; (2) composition model; and (3) physicochemical model. Based on those, the server classifies the sequences as AVP to potential antiviral peptides and non-AVP to non-potential antiviral peptides.

After the design, the best sequences selected by AVPpred were also run in the iAMPpred tool (http://cabgrid.res.in:8080/amppred/) (Meher et al., 2016) to calculate the probability of the sequences selected by AVPpred to be antiviral. The best sequences based on antiviral potential prediction were selected and characterized by physicochemical and biological properties using the iAMPpred tool.

The PEPFold server (https://bioserv.rpbs.univ-paris-diderot.fr/services/PEP-FOLD3/), a widely used computational tool to predict three-dimensional (3D) structures of linear peptides between 5 and 50 amino acids (Shen et al., 2014), was employed to build the 3D structure of ACE-2-derived peptides. The Pymol program was employed to evaluate the peptides' 3D structures and their interaction with the ACE2 human protein.

2.2. Molecular docking (MD) assays

FRODOCK 3.12 (http://frodock.chaconlab.org/) (Ramírez-Aportela et al., 2016), one of the best servers for peptide–-protein interaction, was used to perform all blind molecular docking assays. The peptides with the highest potential were chosen based on the docking score and repetition of poses in the output.

2.3. Molecular dynamic simulation

The complexes generated by the molecular docking tests were minimized and balanced to stabilize them before the

molecular dynamic assays. The force field of all OPLS-AA/L atoms (Moal & Bates, 2010; Robertson et al., 2015) was used to perform the topology, after which a 2-nm cubic box was created. Then, the SPC/E model of water was used for solvation of the box, the systems were neutralized, and the Na + e Cl- ions were added at a concentration of 0.15 M. The minimization was performed until it reached negative potential energy and the lower maximum force of 1000 kJ mol^{-1} nm^{-1}. The pressure and temperature balance was performed to 100 ps. Subsequently, molecular dynamic simulations were performed for 100 ns, and the resulting structures were used for the further analyses.

2.4. Interface analysis of the complexes formed between S-RBD and the studied peptides

The protein interactions calculator (PIC) server was used to analyze the interface interactions of the complexes. The PIC server (http://pic.mbu.iisc.ernet.in/) also determines the accessible surface area and distance of a residue from the protein's surface based on analysis of a set of 3 D structure coordinates. The PyMOL software, a molecular graphics tool widely used for three-dimensional visualization of molecules, was used to generate 3 D figures and perform RMSD calculations. The Ligplot software (Laskowski & Swindells, 2011) was used to generate 2 D figures with the respective representations of hydrophobic interactions and hydrogen bonds.

2.5. Quantum biochemistry calculation

This was performed according to a protocol established previously (Zhang & Zhang, 2003). Molecular fractionation with conjugate caps (MFCC) was carried out to calculate the full quantum mechanical interaction energies between two pairs of specific amino acid residues (Ri and Rj) involving the studied peptides and SARS-CoV-2 Mpro, as follows, based on the work of Amaral et al. (2020):

$$E(R_i - R_j) = E(C_{i-1}R_iC_{i+1} + C_{j-1}R_jC_{j+1}) - E(C_{i-1}R_iC_{i+1} + C_{j-1}C_{j+1}) - E(C_{i-1}C_{i+1} + C_{j-1}R_jC_{j+1}) + E(C_{i-1}C_{i+1} + C_{j-1}C_{j+1})$$

where E($C_{i\text{-}1}$ R_i C_{i+1} + $C_{j\text{-}1}$ R_j C_{j+1}), the first term of the equation, is the total energy of the system formed by the residues Ri and Rj correctly capped; E($C_{i\text{-}1}$ R_i C_{i+1} + $C_{j\text{-}1}$ C_{j+1}), the second term, is the total energy of the system formed by the capped residue Ri and the caps of the residue Rj; the third term, E($C_{i\text{-}1}$ C $_{i+1}$ + $C_{j\text{-}1}$ R_j C_{j+1}), represents the total energy of the system formed by the capped residue Rj and the caps of the residue Ri; and the last term, E($C_{i\text{-}1}$ C_{i+1} + $C_{j\text{-}1}$ C_{j+1}), accounts for the system's total energy, formed by the caps of both residues Ri and Rj. The caps $C_{i\text{-}1}$(C_{i+1}) and $C_{j\text{-}1}$(C_{j+1}) are made from the residues covalently bound to the amine (carboxyl) groups of Ri and Rj. In the MFCC method used, all interaction between amino acid residues of the studied peptides and SARS-CoV-2 Mpro separated from each other within an 8 Å range were calculated, considering a dielectric function approach of 40 ($\varepsilon = 40$) for all interactions. The structural files (PDB format) obtained after molecular dynamic simulation and MFCC were used as inputs for density functional theory (DFT) calculations with DMOL^3 (Delley, 2000).

3. Results

3.1. ACE2-derived peptide design

The AVPpred was set up to use the ACE2 sequence to produce peptides with 10, 15 and 20 amino acid residues. There were 100, 80 and 79 peptides generated, with 10, 15 and 20 amino acid residues, respectively, for a total of 259 peptides (Supplementary Tables S1–S3). Of those, AVPpred selected four peptides with antiviral potential, which were named ACE2-Dev-PepI, ACE2-Dev-PepII, ACE2-Dev-PepIII and ACE2-Dev-PepIV (Table 1).

As summarized in Table 1, all peptides were cationic, with positive charges ranging from +1 to +3, hydrophobic ratio from 45 to 60% and calculated molecular mass ranging from 1802.16 to 2587.14. Regarding biological properties, the iAMPpred tool revealed antiviral potentials of 80, 75, 63 and 35, respectively, for ACE2-Dev-PepI, ACE2-Dev-PepII, ACE2-Dev-PepIII and ACE2-Dev-PepIV (Table 2), corroborating the analysis of AVPpred. The *in silico* analyses revealed that all peptides had no hemolytic, allergenic or toxic potential (Table 2). This is interesting because designing peptides from the ACE2 human receptor can reduce any collateral effect.

In silico analyses also revealed that all peptides possibly interacted with DNA and RNA (Table 2). The interaction with RNA is particularly interesting because SARS-CoV-2 and other coronaviruses have RNA as genetic material. Looking forward to clinical application, we tested the resistance of these peptides in the intestinal-like environment. ACE2-Dev-PepIII presented a half-life of 0.021 s, indicating low stability, which means that enzymes promptly digest it. ACE2-Dev-PepIV showed normal stability, as indicated by the half-life of 0.614 s. ACE2-Dev-PepI and ACE2-Dev-PepII presented high stability, with half-life values of 3.461 and 1.669 s, respectively (Table 2). These values indicate the possibility of oral administration of the last two peptides.

The PEPFold server predicted that all ACE2-dev peptides contain long helices as secondary structures (Supplementary Figure S1). The Ramachandran plot (Table 1) revealed 98%, 99%, 95% and 99% of favorable regions for helix formation, respectively, for ACE2-Dev-PepI, ACE2-Dev-PepII, ACE2-Dev-PepIII and ACE2-Dev-PepIV (Table 1).

3.2. Molecular docking and dynamic simulations revealed interaction and stabilization between the ACE2-derived peptides and S-RBD

Given the large size of the entire SARS-CoV-2 S protein, many research groups have chosen to perform molecular docking and dynamic simulations using only the RBD structure (Amaral et al., 2020; Delley, 2000; Wu et al., 2020; Zhang & Zhang, 2003). Here, we followed the same approach. Molecular docking analyses showed that all ACE2-derived peptides interacted with S-RBD in the same region, with

Table 1. Physicochemical properties of the ACE2-derived peptides.

Properties/peptides	ACE2-Dev-Pep-I	ACE2-Dev-Pep-II	ACE2-Dev-Pep-III	ACE2-Dev-Pep-IV
Sequence	CLPAHLLGDMWGRFW	MRQYFLKVKNQMILF	PFTYMLEKWRWMVFKGEIPK	CLPAHLLGDMWGRFWTNLYS
[a]pI	6.7	10.3	9.5	6.3
[b]Calculated molecular mass (Da)	1802.16	1959.45	2587.14	2380.78
[b]Hydrophobic ratio (%)	60	53	45	50
[b]Net charge	+1	+3	+2	+1
[c]Ramachandran plot (%)	98	99	95	99
[d]Tm	0.470	0.335	0.223	0.537
[d]sOPEP	−32.2	−29.49	−48.60	−46.57

[a]Calculated by using the ProtParam tool (https://web.expasy.org/protparam/protpar-ref.html).
[b]Data generated by the antimicrobial peptide database (APD, http://aps.unmc.edu/AP/).
[c]Calculated by using the program Rampage (http://mordred.bioc.cam.ac.uk/~rapper/rampage.php).
[d]Calculated by using the PepFOLD 3.0 server (http://mobyle.rpbs.univ-paris-diderot.fr/cgi-bin/portal.py#forms::PEP-FOLD).

Table 2. ACE2-derived peptide properties obtained by bioinformatic analyses.

Properties/peptides	ACE2-Dev-Pep-I	ACE2-Dev-Pep-II	ACE2-Dev-Pep-III	ACE2-Dev-Pep-IV
[a]Allergic potential	No	No	No	No
[b]Hemolytic potential (%)	0	0	1	0
[c]Toxic potential	Non-toxic	Non-toxic	Non-toxic	Non-toxic
[d]Antiviral prediction	Yes	Yes	Yes	Yes
[e]Antiviral potential (%)	80	75	63	35
[f]DNA binding	Yes	Yes	Yes	Yes
[g]RNA binding	Yes	Yes	Yes	Yes
[h]Half-life	3.461	1.669	0.021	0.614
[i]Stability	High	High	Low	Normal

[a]The allergic potential was calculated using the antigenic prediction tool (http://imed.med.ucm.es/Tools/antigenic.pl).
[b]The hemolytic potential was calculated by the HemoPI tool (http://crdd.osdd.net/raghava/hemopi/submitfreq.php?ran=44366).
[c]The toxin potential was calculated using ToxinPred (http://crdd.osdd.net/raghava/toxinpred/design.php).
[d]The antiviral potential was calculated using the AVpred (http://crdd.osdd.net/servers/avppred/).
[e]The antiviral potential was calculated using the iAMPpred tool (http://cabgrid.res.in:8080/amppred/).
[f]The DNA-binding potential was assessed by using DNAbinder (http://crdd.osdd.net/cgibin/dnabinder/valid1.pl).
[g]The RNA-binding potential was assessed by using RNApred (http://crdd.osdd.net/raghava/rnapred/submit.html).
[h]The half-life in seconds was calculated using the half-life prediction tool (http://crdd.osdd.net/raghava/hlp/help.html), which predicts the proteolytic activity in the intestinal-like environment.
[i]Stability was calculated using the half-life prediction tool (http://crdd.osdd.net/raghava/hlp/help.html). Half-life < 0.1 s means low stability; half-life from 0.1 to 1.0 s means normal stability; and half-life > 1.0 s means high stability.

different scores, as revealed by the FRODDOCK server (Figure 1). The peptides ACE2-Dev-PepI, ACE2-Dev-PepII, ACE2-Dev-PepIII, and ACE2-Dev-PepIV presented scores of 3003.43, 2909.40, 2829.25, and 3251.67 kj.mol^{-1}, respectively.

Molecular dynamic simulation showed the stabilization of the complexes formed by ACE2-Dev-PepI, ACE2-Dev-PepII, ACE2-Dev-PepIII, and ACE2-Dev-PepIV with S-RBD after assay of 30 ns, remaining stable up to 100 ns, with RMSD variations below 1 Å after 30 ns (Figure 2). The stable conformation obtained from each MD simulation was used to perform all further analyses.

3.3. Interaction between S-RBD and ACE2-Dev-PepI

The most relevant interactions among the amino acid residues from S-RBD and ACE2-Dev-PepI were by: Tyr^{489}, Tyr^{473}, Tyr^{489}, Phe^{456}, Ala^{475}, Tyr^{489}, Leu^{455}, Lys^{458}, Tyr^{489}, and Ala^{475} of RBD with Phe^{14}, Trp^{15}, Trp^{11}, Trp^{15}, Phe^{14}, Trp^{15}, Trp^{11}, Trp^{15}, Met^{10},\ and Trp^{15} of ACE2-Dev-PepI. The interaction energies of interaction were, respectively, −7.40, −7.22, −6.65, −5.54, −5.41, −4.57, −3.11, −2.90, −2.86 and −2.72 kcal.mol^{-1}, with distances of 1.69, 1.76, 2.63, 2.54, 2.17, 2.40, 2.26, 4.70, 2.04 and 2.65 Å, respectively. All existing interactions up to a distance of 8 Å are reported in Supplementary Table S4.

The complex ACE2-Dev-PepI::S-RBD is supported by many interactions, such as hydrophobic and aromatic–aromatic interactions, along with hydrogen bonds (Figure 3(A,B,D)). The hydrophobic interactions were with residues Tyr^{489}, Leu^{455}, Tyr^{489}, Ala^{475}, Tyr^{489}, Phe^{456}, Tyr^{473}, and Tyr^{489} of S-RBD with Met^{10}, Trp^{11}, Trp^{11}, Phe^{14}, Phe^{14}, Trp^{15}, Trp^{15} and Trp^{15} of ACE2-Dev-PepI (Figure 3(B,D)). The hydrogen bonds occurred between residues Phe^{489} and Tyr^{489} of S-RBD and residues Met^{10} and Phe^{14} of ACE2-Dev-PepI (Figure 3(A,B,D)). The aromatic–aromatic interactions were formed between residues Tyr^{489} and Phe^{456} of S-RBD and residues Trp^{11} and Trp^{15} of ACE2-Dev-PepI (Figure 3(A,D).

Met10, Trp11, Phe14 and Trp15 were the most relevant amino acid residues of ACE2-Dev-PepI in the interaction with S-RBD, with respective interaction energies of −6.78, −15.40, −17.24 and −23.81 kcal.mol^{-1} (Figure 3(C)).

3.4. Interaction of S-RBD with ACE2-Dev-PepII

Regarding the complex ACE2-Dev-PepII::S-RBD, interactions occurred between residues Arg^{403}, Glu^{484}, Leu^{492}, Tyr^{473}, Gln^{493}, Phe^{456}, Leu^{455}, Tyr^{505}, Tyr^{489}, Leu^{455} and Phe^{490} of S- RBD, and residues Phe^{15}, Lys^{9}, Lys^{9}, Phe^{5}, Lys^{9}, Phe^{5}, Val^{8}, Phe^{15}, Leu^{6}, Lys^{9} and Lys^{9} of ACE2-Dev-PepII. The interaction energies of those interactions were, respectively, −13.81, −11.00, −5.14, −4.98, −4.61, −4.34, −4.23, −3.91, −3.61, −3.21 and −2.93 kcal.mol^{-1} with distances of 1.63, 1.57, 2.18, 2.39, 2.85, 2.57, 2.39, 2.33, 2.31, 2.35 and 2.15 Å. The ACE2-Dev-PepII::S-RBD complex presented a repulsive interaction between Arg^{403} of S-RBD and Leu^{14} of ACE2-Dev-PepII, with interaction energy

COLOR Online / B&W in Print

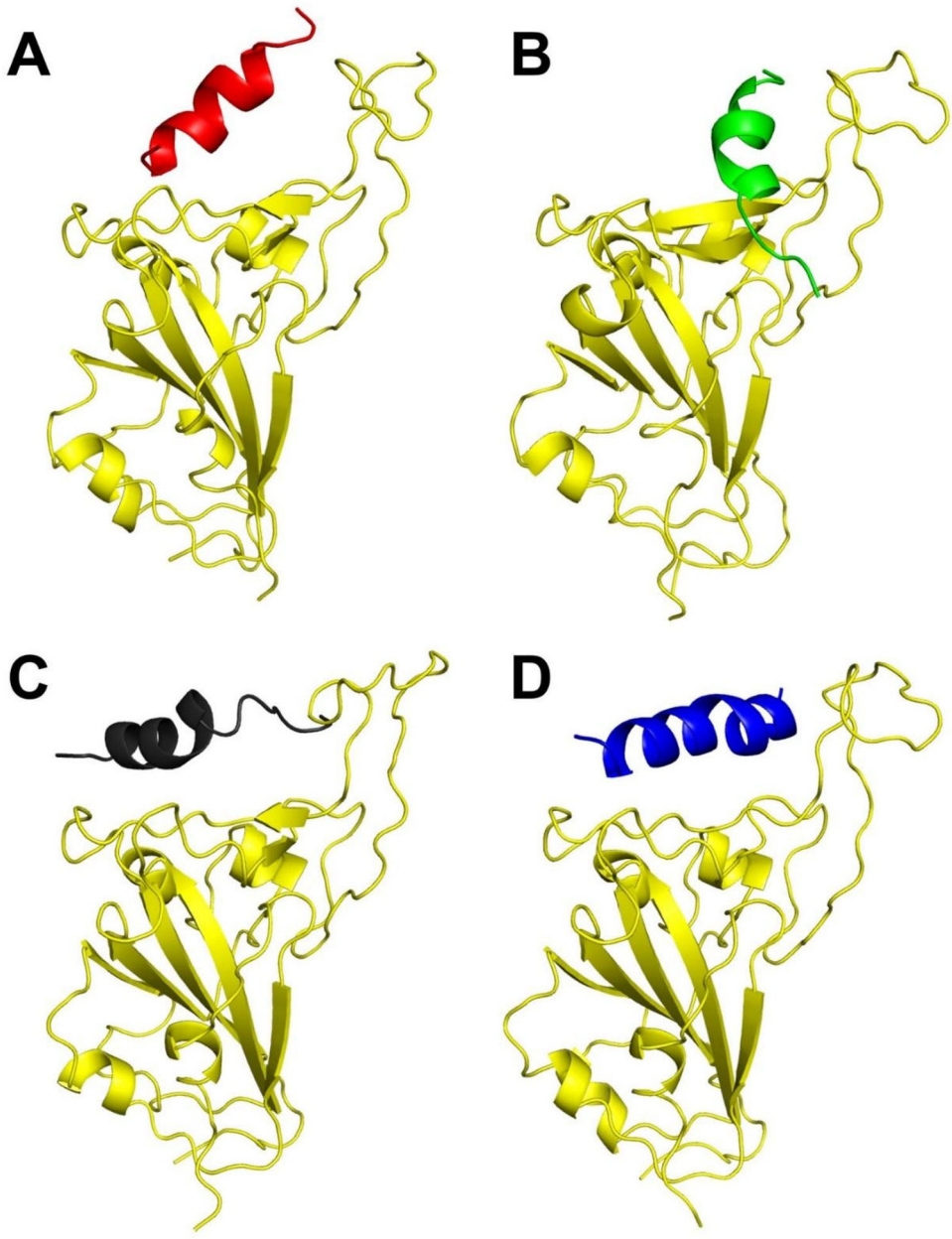

Figure 1. Molecular docking revealed that peptides derived from ACE2 human protein can interact with SARS-CoV-2 RBD. The target SARS-CoV-2 RBD is represented in cartoon yellow and ACE2-Dev-PepI in red (A), ACE2-Dev-PepII in green (B), ACE2-Dev-PepIII in black (C) and ACE2-Dev-PepIV in blue (D).

of +1.47 kcal.mol^{-1} and distance of 5.09 Å.Supplementary Table S5 summarizes all interactions between ACE2-Dev-PepII and SARS-CoV-2 RBD up to a distance of 8 Å.

The interaction between ACE2-Dev-PepII and S-RBD occurred through hydrophobic, ionic, aromatic-aromatic, cation–pi and hydrogen bonds (Figure 4(A–C)). Tyr^{489}, Phe^{456}, Phe^{456}, Tyr^{473}, Ala^{475}, Ala^{475}, Tyr^{489}, Leu^{455}, Phe^{456}, Pro^{491}, Tyr^{453}, Leu^{455} and Tyr^{505} of S-RBD had hydrophobic interactions with residues Met^{1}, Tyr^{4}, Phe^{5}, Phe^{5}, Phe^{5}, Leu^{6}, Leu^{6}, Val^{8}, Val^{8}, Val^{8}, Met^{12}, Met^{12}, Phe^{15} of ACE2-Dev-PepII peptide (Figure 4(B,C)). Hydrogen bonds occurred between residues Phe^{490}, Leu^{492}, Glu^{484} and Tyr^{453}of S-RBD and residues Lys^{9}, Lys^{9}, Lys^{9} and Met^{12} of ACE2-Dev-PepII (Figure 4(A–C)).

Ionic interaction occurred between the Glu^{484} residue of S-RBD and Lys^{9} residue of ACE2-Dev-PepII. Four cation–pi interactions happened between residues Lys^{458}, Arg^{403}, Tyr^{489} and Phe^{490} of S-RBD and residues Phe^{5}, Phe^{15}, Lys^{9} and Lys^{9}of ACE2-Dev-PepII (Figure 4(C)). Finally, the Phe^{456}, Phe^{456}, Tyr^{473} and Tyr^{505}residues of S-RBD had aromatic–aromatic interactions with the residues Tyr^{4}, Phe^{5}, Phe^{5} and Phe^{15} of ACE2-Dev-PepII (Figure 4(C)).

The most relevant amino acid residues of ACE2-Dev-PepII that interacted with S-RBD were Phe5, Leu6, Val8, Lys9, Met12 and Phe15 with the interaction energies of −16.11, −12.78, −9.23, −31.58, −5.95 and −20.79 kcal.mol^{-1}, respectively (Figure 4(D)).

3.5. Interaction between S-RBD and ACE2-Dev-PepIII

In the complex formed between ACE2-Dev-PepIII::S-RBD, the main interactions were by residues Lys^{417}, Arg^{408}, Tyr^{453}, Glu^{406}, Tyr^{489}, Leu^{455}, Gln^{493}, Gln^{493}, Gln^{493} and Phe^{456} of S-

RBD with residues Glu[7], Phe[2], Arg[10], Arg[10], Phe[14], Phe[14], Trp[9], Val[13], Arg[10] and Phe[14] of ACE2-Dev-PepIII. The interaction energies were, respectively, −11.04, −8.78, −5.04, −4.88, −3.90, −3.81, −3.34, −3.24, −3.22 and −3.04 kcal.mol^{-1} and distances of 1.59, 2.53, 1.89, 4.01, 2.48, 2.23, 2.01, 2.66, 2.51, 2.62 Å, respectively. Repulsive interactions occurred between residues Glu[406] and Arg[403] of SARS-CoV-2 RBD and residues Glu[7] and Arg[10] of ACE2-Dev-PepIII, with interaction energies of +1.42 and +1.98 kcal.mol^{-1}, respectively. All interactions between ACE2-Dev-PepIII and SARS-CoV-2 RBD up to a distance of 8 Å are reported in Supplementary Table S6.

COLOR Online / B&W in Print

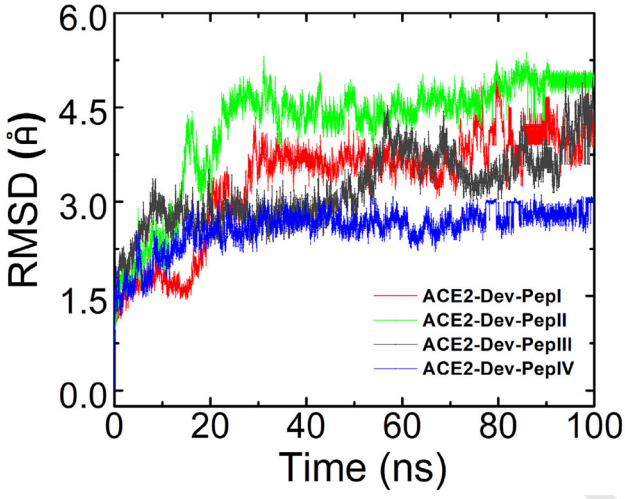

Figure 2. Molecular dynamic simulations obtaining stable structures. The complexes formed between the four peptides derived from ACE2 and SARS-CoV-2 were examined by molecular dynamics, and stable structures were obtained after 100 ns. Each RMSD variation demonstrated stability during the simulation after 30 ns.

ACE2-Dev-PepIII interacted with S-RBD through hydrophobic, ionic, aromatic-aromatic, cation–pi interactions and hydrogen bonds. The residues Tyr[505], Tyr[505], Leu[455], Leu[455], Phe[456] and Tyr[489] of S-RBD were involved in hydrophobic interactions with Met[5], Trp[9], Val[13], Phe[14], Phe[14] and Phe[14] of ACE2-Dev-PepIII (Figure 5(B,D)). Tyr505, Phe456 and Tyr489 of S-RBD, and Trp9, Phe14 and Phe14 of ACE2-Dev-PepIII (Figure 5(A,D)) drove aromatic–aromatic interactions. Hydrogen bonds occurred between Gln[493], Gln[493], Tyr[453] and Lys[417] residues of S-RBD and the Trp[9], Trp[9], Arg[10] and Glu[7] residues of ACE2-Dev-PepIII (Figure 5(A,B,D)).

Phe[2], Leu[6], Glu[7], Trp[9], Arg[10], Val[13], Phe[14] and Lys[15] were the main amino acid residues of ACE2-Dev-PepIII that interacted with S-RBD, with interaction energy values of −13.98, −6.13, −11.52, −9.74, −14.52, −7.07, −13.85 and −4.38 kcal.mol^{-1}.

3.6. Interaction between S-RBD and ACE2-Dev-PepIV

The main interactions between amino acid residues were driven by Tyr[449], Gln[493], Tyr[489], Phe[490], Leu[455], Gln[498], Gln[498], Phe[456], Phe[456], Phe[456] and Leu[455] of S-RBD and residues Leu[18], Trp[11], Leu[7], Trp[11], Leu[6], Leu[18], Asn[17], Leu[7], Pro[3], Leu[6] and Leu[7] of ACE2-Dev-PepIV. The interaction energies were −5.27, −5.07, −4.99, −4.14, −4.05, −3.91, −3.85, −3.82, −3.40, −3.04 and −3.03 kcal.mol^{-1}, with distances of 2.22, 2.92, 2.18, 2.25, 2.25, 3.43, 1.71, 2.22, 2.51, 2.12 and 2.22 Å, respectively. The repulsive interaction was between the residue Gly[485] of S-RBD and Leu[7] of ACE2-Dev-PepIV, with the interaction energy of +0.54 kcal.mol^{-1}. All interactions between ACE2-Dev-PepIV and SARS-CoV-2 RBD up to a distance of 8 Å are reported in Supplementary Table S7.

COLOR Online / B&W in Print

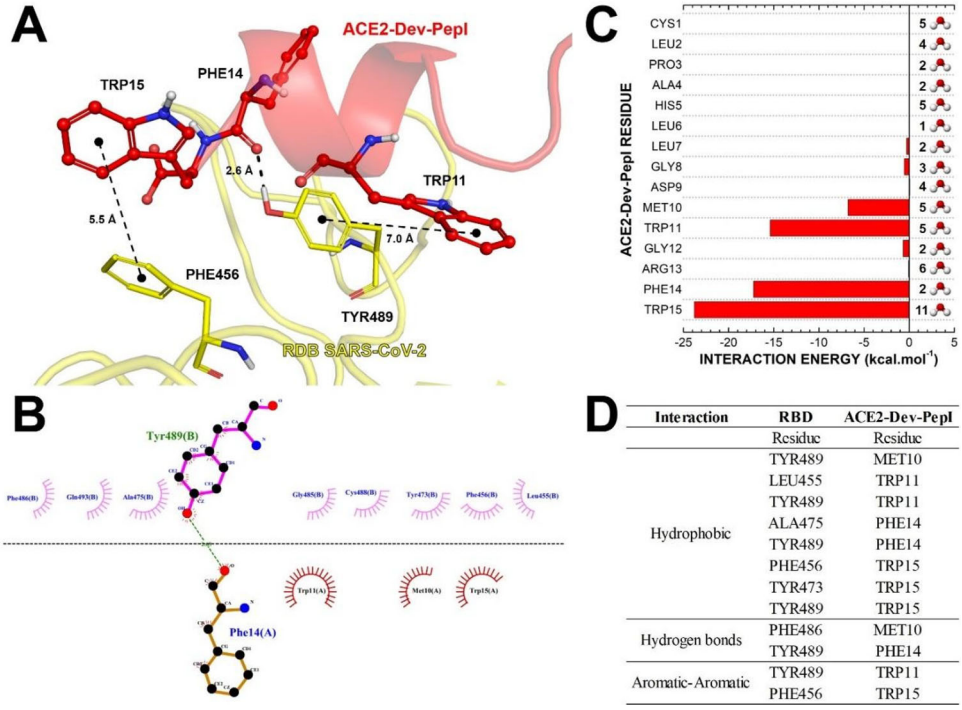

Interaction	RBD Residue	ACE2-Dev-PepI Residue
Hydrophobic	TYR489	MET10
	LEU455	TRP11
	TYR489	TRP11
	ALA475	PHE14
	TYR489	PHE14
	PHE456	TRP15
	TYR473	TRP15
	TYR489	TRP15
Hydrogen bonds	PHE486	MET10
	TYR489	PHE14
Aromatic-Aromatic	TYR489	TRP11
	PHE456	TRP15

Figure 3. Energies and interaction between SARS-CoV-2 RBD (yellow) and ACE2-Dev-PepI (red). A and B represent the 3D interactions and 2D interactions, respectively. C represents the individual energy contribution of each amino acid residue of ACE2-Dev-PepI, and D denotes all interactions between SARS-CoV-2 RBD and ACE2-Dev-PepI.

COLOR Online / B&W in Print

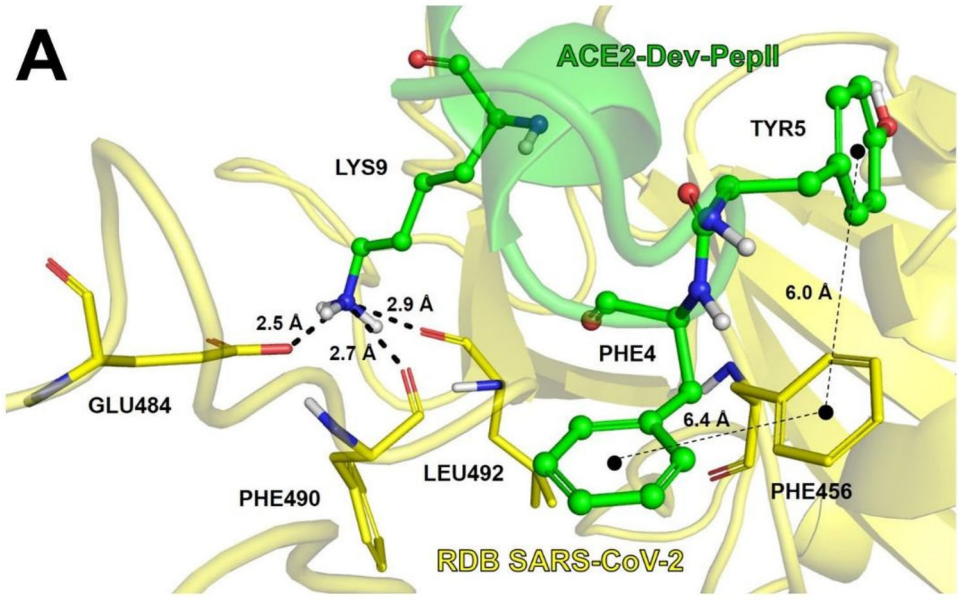

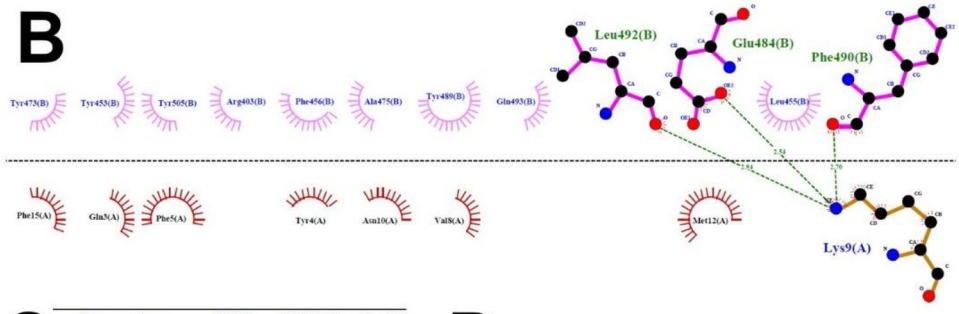

C

Interaction	RBD Residue	ACE2-Dev-PepII Residue
Hydrophobic	TYR489	MET1
	PHE456	TYR4
	PHE456	PHE5
	TYR473	PHE5
	ALA475	PHE5
	ALA475	LEU6
	TYR489	LEU6
	LEU455	VAL8
	PHE456	VAL8
	PRO491	VAL8
	TYR453	MET12
	LEU455	MET12
	TYR505	PHE15
Hydrogen bonds	PHE490	LYS9
	LEU492	LYS9
	GLU484	LYS9
	TYR453	MET12
Ionic	GLU484	LYS9
Aromatic-Aromatic	PHE456	TYR4
	PHE456	PHE5
	TYR473	PHE5
	TYR505	PHE15
Cation-Pi	LYS458	PHE5
	ARG403	PHE15
	TYR489	LYS9
	PHE490	LYS9

D

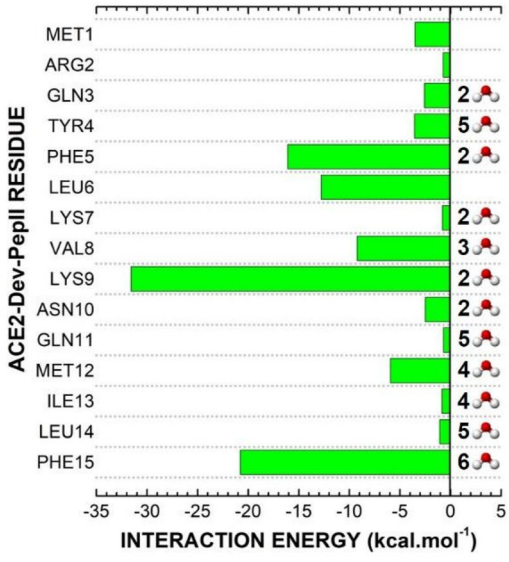

Figure 4. Energies and interaction between SARS-CoV-2 RBD (yellow) and ACE2-Dev-PepII (green). A and B represent the 3D interactions and 2D interactions, respectively. C denotes all interactions between SARS-CoV-2 RBD and ACE2-Dev-PepII, and D represents the individual energy contribution of each amino acid residue of ACE2-Dev-PepII.

Hydrophobic, and aromatic–aromatic interactions along with hydrogen bonds are the interactions that stabilize the ACE2-Dev-PepIV::S-RBD complex. Hydrophobic interactions occurred between ACE2-Dev-PepIV and residues Phe^{456}, Phe^{456}, Ala^{475}, Tyr^{489}, Tyr^{489}, Tyr^{421}, Leu^{455}, Phe^{456}, Leu^{455}, Phe^{456}, Tyr^{473}, Tyr^{489}, Pro^{491}, Leu^{455}, Leu^{455}, Phe^{490}, Tyr^{453}, Leu^{455} and Tyr^{449} of S-RBD (Figure 6(B,D). Eight hydrogen bonds occurred between residues Phe^{490}, Gln^{493}, Gln^{493}, Gln^{493}, Gln^{498}, Gln^{498}, Gln^{498} and Gln^{498} of S-RBD and residues Trp^{11}, Trp^{15}, Phe^{14}, Phe^{14}, Asn^{17}, Asn^{17}, Tyr^{19} and Tyr^{19} of ACE2-Dev-PepIV, respectively (Figure 6(A,B,D)). Aromatic–aromatic interaction occurred between $Phe^{490}$of S-

COLOR Online / B&W in Print

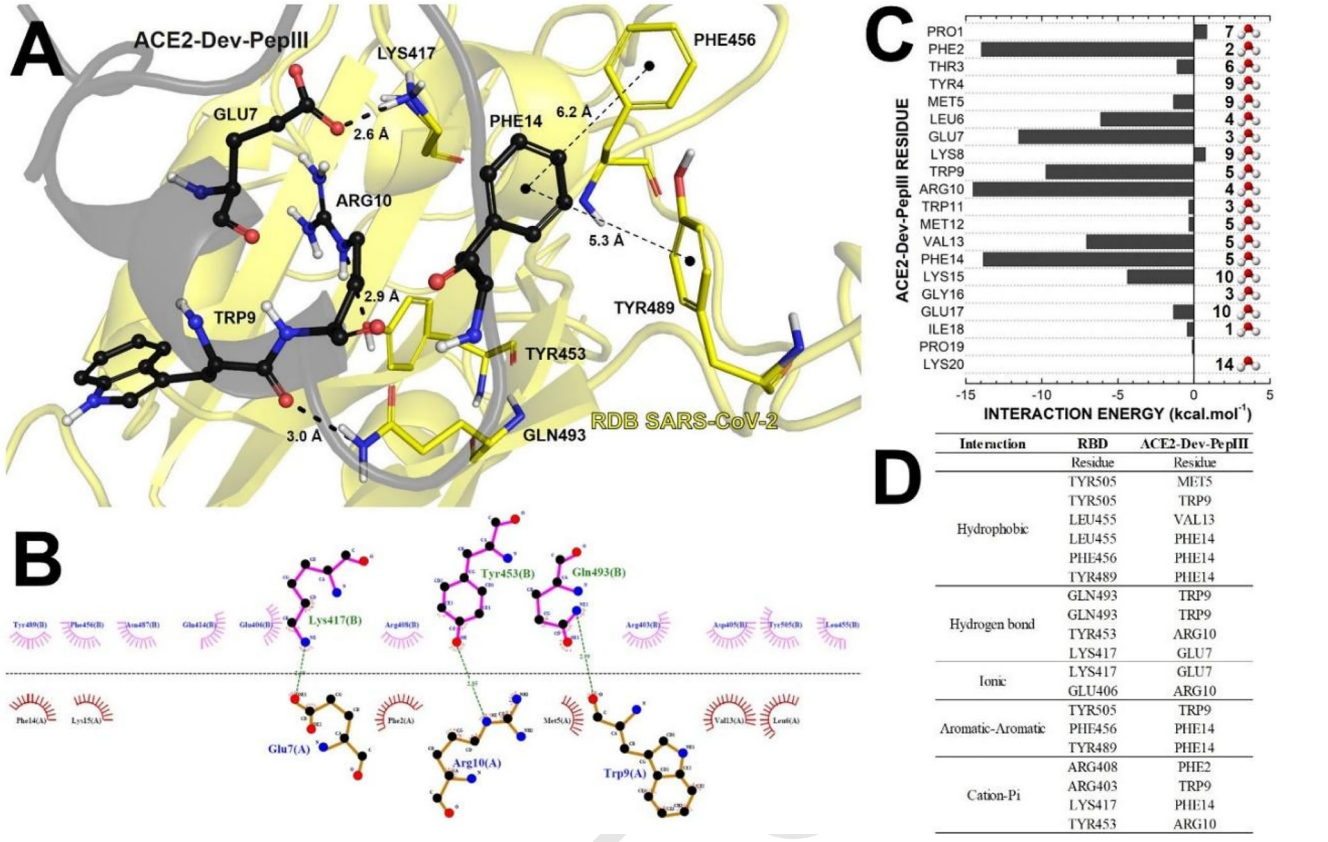

Interaction	RBD Residue	ACE2-Dev-PepIII Residue
Hydrophobic	TYR505	MET5
	TYR505	TRP9
	LEU455	VAL13
	LEU455	PHE14
	PHE456	PHE14
	TYR489	PHE14
Hydrogen bond	GLN493	TRP9
	GLN493	TRP9
	TYR453	ARG10
	LYS417	GLU7
Ionic	LYS417	GLU7
	GLU406	ARG10
Aromatic-Aromatic	TYR505	TRP9
	PHE456	PHE14
	TYR489	PHE14
Cation-Pi	ARG408	PHE2
	ARG403	TRP9
	LYS417	PHE14
	TYR453	ARG10

Figure 5. Energies and interaction between SARS-CoV-2 RBD (yellow) and ACE2-Dev-PepIII (black). A and B represent the 3D interactions and 2D interactions, respectively. C represents the individual energy contribution of each amino acid residue of ACE2-Dev-PepIII, and D denotes all interactions between SARS-CoV-2 RBD and ACE2-Dev-PepIII.

RBD and Trp[11] residue of ACE2-Dev-PepIV, respectively (Figure 6(A,D)).

Pro[3], Leu[6], Leu[7], Trp[11], Phe[14], Asn[17] and Leu[18] were the main amino acid residues of ACE2-Dev-PepIV that interacted with S-RBD, with interaction energies of −8.55, −10.54, −19.27, −16.08, −10.03, −8.26, −14.77 kcal.mol^{-1} (Figure 6(C)).

3.7. Quantum biochemistry description

ACE2-Dev-PepI mainly interacted with residues Tyr[489], Ala[475], Tyr[473], Phe[456], Leu[455], Asn[487] and Lys[458] of S-RBD, with interaction free energies of −21.54, −8.78, −7.23, −6.27, −3.91, −3.17 and −2.90 kcal.mol^{-1}, respectively (Figure 7(A)). The ACE2-Dev-PepII peptide interacted primarily with residues Arg[403], Glu[484], Gln[493], Leu[455], Phe[456], Tyr[489], Tyr[473], Leu[492], Pro[491], Asn[487], Tyr[505], Ala[475] and Phe[490 94] of S-RBD, with interaction energies of −12.67, −11.03, −10.64, −10.23, −9.92, −9.42, −7.04, −5.29, −4.87, −4.42, −4.07, −3.78 and −3.43 kcal.mol^{-1}, respectively (Figure 7(B)). The ACE2-Dev-PepIII peptide mainly interacted with the amino acid residues Lys[417], Gln[493], Arg[408], Leu[455], Tyr[453], Glu[406], Tyr[489], Gln[409], Phe[456], Tyr[505] and Asp[405] of the S-RBD, with interaction energies of −12.13, −10.56, −9.40, −8.79, −6.08, −5.02, −4.85, −3.92, −3.55, −3.31 and −3.31 kcal.mol^{-1}, respectively (Figure 7(C)). ACE2-Dev-PepIV mainly interacted with residues Leu[455], Phe[456], Gln[498], Gln[493], Tyr[489], Tyr[449], Phe[490], Ser[494], Pro[491], Tyr[453], Ala[475] and Gly[496] of S-RBD, with interaction energies of −14.65, −13.38, −11.44, −10.72, −10.58, −6.60, −6.22, −4.19, −4.07, −3.22, −3.14 and −3.12 kcal.mol^{-1}, respectively (Figure 7(D)).

The ACE2-Dev-PepII and ACE2-Dev-PepIV peptides had the lowest interaction energy, of −112.8 and −113.9 kcal. mol^{-1}, respectively, with S-RBD, so they have highest potentials to inhibit the interaction between S-RBD and ACE2 receptor. ACE2-Dev-PepI and ACE2-Dev-PepIII presented total interaction energies, E(t), equal to −64.9 and −84.6 kcal.mol^{-1}, respectively (Figure 8). Energy convergence was observed in all complexes formed between ACE2-derived peptides and S-RBD after a distance greater than 6 Å, with minimal variations seen after that distance (Figure 8).

3.8. ACE2-derived peptides induced wrong interaction between S-RBD and the ACE2 receptor

All ACE2-derived peptides induced incorrect binding of S-RBD with the ACE2 receptor. The redocking confirmed the reliability of the docking tool, since the conformation generated by the redocking (Figure 9(B)) was similar to the crystal structure used as control (Figure 9(A)). When S-RBD was bound to ACE2-Dev-PepI, ACE2-Dev-PepII, ACE2-Dev-PepIII or ACE2-Dev-PepIV peptides could not recognize the ACE2 receptor in the correct conformation (Figure 9(C–F)). The ACE2 region that generally interacts with S-RBD was no longer able to interact in the correct conformation with S-RBD.

COLOR Online / B&W in Print

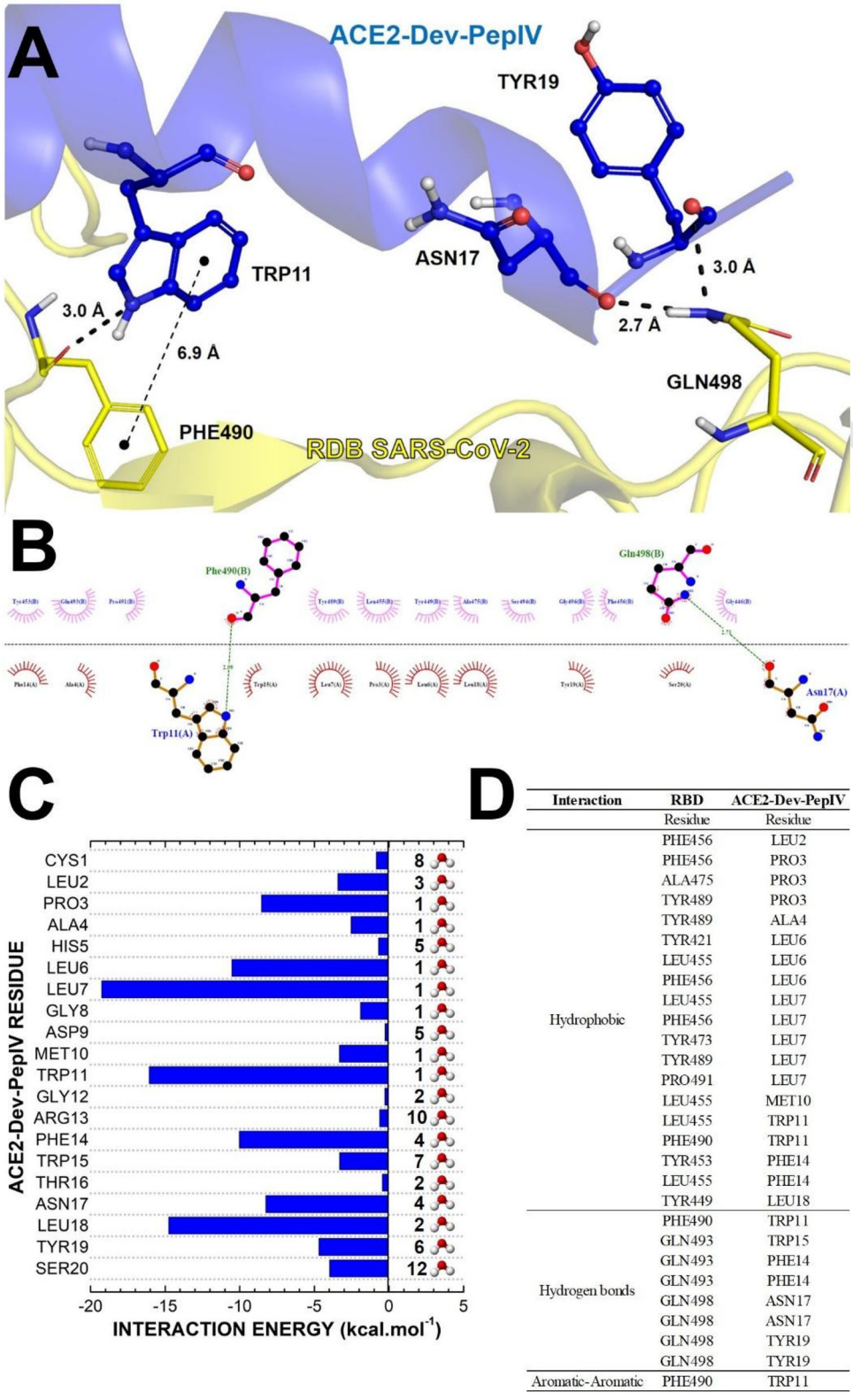

D

Interaction	RBD Residue	ACE2-Dev-PepIV Residue
Hydrophobic	PHE456	LEU2
	PHE456	PRO3
	ALA475	PRO3
	TYR489	PRO3
	TYR489	ALA4
	TYR421	LEU6
	LEU455	LEU6
	PHE456	LEU6
	LEU455	LEU7
	PHE456	LEU7
	TYR473	LEU7
	TYR489	LEU7
	PRO491	LEU7
	LEU455	MET10
	LEU455	TRP11
	PHE490	TRP11
	TYR453	PHE14
	LEU455	PHE14
	TYR449	LEU18
Hydrogen bonds	PHE490	TRP11
	GLN493	TRP15
	GLN493	PHE14
	GLN493	PHE14
	GLN498	ASN17
	GLN498	ASN17
	GLN498	TYR19
	GLN498	TYR19
Aromatic-Aromatic	PHE490	TRP11

Figure 6. Energies and interaction between SARS-CoV-2 RBD (yellow) and ACE2-Dev-PepIV (blue). A and B represent the 3D interactions and 2D interactions, respectively. C represents the individual energy contribution of each amino acid residue of ACE2-Dev-PepIV, and D denotes all interactions between SARS-CoV-2 RBD and ACE2-Dev-PepIV.

4. Discussion

The development of vaccines is the most crucial measure to block SARS-CoV-2 spread and infection. Even though many research groups worldwide are rushing to develop an efficient vaccine against SARS-CoV-2, an undesirable problem has arisen. Some studies have shown the immunological memory mediated by IgGs anti-SARS-CoV-2 is brief, only around three months. Besides that, there are reports of patients infected twice by SARS-CoV-2 (Diamond & Pierson, 2020; Tay et al., 2020). This problem related to immunity

COLOR Online / B&W in Print

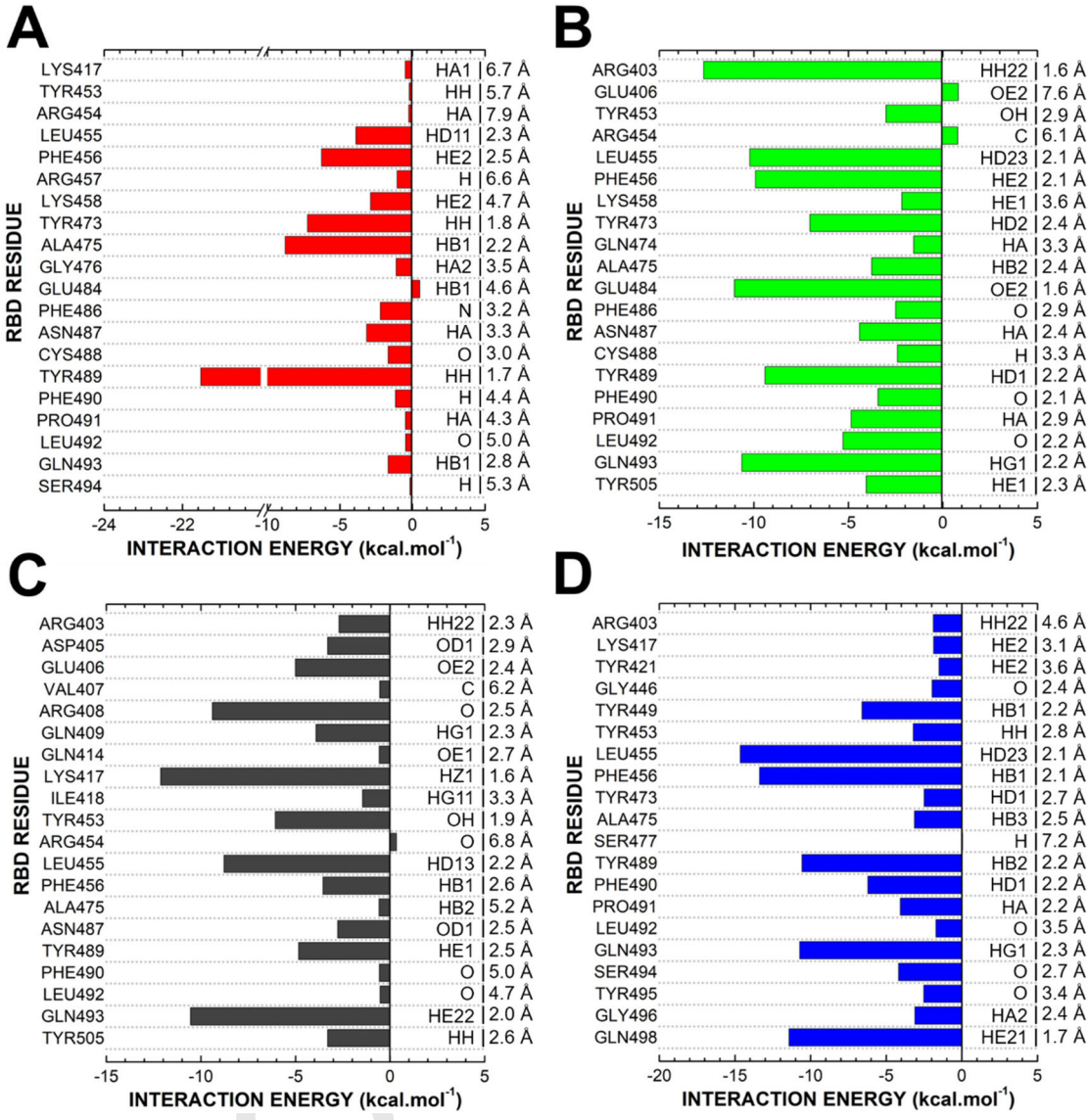

Figure 7. Binding site, interaction energy and residue domain (BIRD) panel showing the MFCC interaction energies between the central amino acid residues of SARS-CoV-2 RBD and ACE2-derived peptides. ACE2-Dev-PepI (A), ACE2-Dev-PepII (B), ACE2-Dev-PepIII (C) and ACE2-Dev-PepIV (D). The minimal distance (Å) between each residue that participates in the interaction is indicated at the right side of the panel. The amino acid residues at the left side of the panel are from SARS-CoV-2 RBD.

offered by the vaccine to SARS-CoV-2 represents a considerable challenge to the world population. Therefore, research for new molecules is imperative to abolish or even attenuate its symptoms.

One approach to develop therapies quickly is repositioning of already available antiviral drugs to treat SARS-CoV-2 (Yan et al., 2020), which has not been successful so far. The most employed way to discover possible alternative compounds against SARS-CoV-2 is computational screening (Diamond & Pierson, 2020; Tay et al., 2020). By employing computational screening, it is possible to choose as target a vital protein to SARS-CoV-2 infection, such as RNA polymerase, a main protease and S protein (Elfiky, 2020; Souza et al., 2020). For instance, Elfiky (Zhang et al., 2020) used molecular docking to test many conventional antiviral drugs such as galidesivir, remdesivir and tenofovir against the RNA polymerase of SARS-CoV-2. In turn, Wu et al. (2020) performed molecular docking simulation of drugs such as antihypertensives, antifungals and anticoagulants against SARS-CoV-2 targets.

The spike glycoprotein of coronaviruses is an essential protein to infection. It has two portions, S1 outside the virus envelope, which is connected to S2, a transmembrane portion attached to the virus envelope. S1 possesses the RBD domain, which interacts with ACE2. After this interaction, the S2 portion is responsible for membrane fusion and virus entry (Hoffmann et al., 2020; Yuan et al., 2017). The S-RBD domain possesses high mutational rates, characterizing it as the most variable region of the coronavirus genome (Wu et al., 2020; Zhou et al., 2020).

In SARS-CoV-like viruses, there are six amino acid residues critical to the interaction between the RBD domain and the ACE2 receptor. The mutations accumulated by SARS-CoV-2 lead to five amino acid residues that are different from in to SARS-CoV. In SARS-CoV, the residues are Tyr^{455}, Leu^{486}, Asn^{494}, Asp^{495}, Tre^{501} and Tyr^{506}. In contrast, in SARS-CoV-2,

the residues are Leu[455], Phe[486], Glu[494], Ser[495], Asn[501] and Tyr[506] (Andersen et al., 2020; Walls et al., 2020). These differences in the SARS-CoV-2 RBD domain allow it to bind to ACE2 with an affinity 20 times higher than SARS-CoV (Andersen et al., 2020). The ACE2 receptor is expressed in different human tissues, such as kidneys, gut, brain, liver, heart and lungs. By using it to enter the cells, SARS-CoV-2 can infect nearly all these tissues, causing SARS-CoV-2 viral sepsis, meaning the virus can infect several tissues at the same time (Li et al., 2020).

Given the importance of interaction between S-RBD and ACE2, several research groups have been seeking molecules that can block this interaction, either by interaction with S-RBD or with the ACE2 receptor, (Choudhary et al., 2020; de Oliveira et al., 2020; Wu et al., 2020). Choudhary et al. (2020) employed molecular dynamic simulations to find ligand molecules that interact with the ACE2 receptor and thus block interaction with SARS-CoV-2 RBD. This can be a two-way road, because by blocking the ACE2 receptor, SARS-CoV-2 cannot recognize it and does not establish infection. However, choosing to block the ACE2 receptor at the same time makes it unavailable to the cells, and hence produces several collateral effects. In a virtual screening, Wu et al. (2020) found a flavonoid from citrus fruit, called hesperidin, which interacted with RBD, blocking its interaction with ACE2. However, hesperidin has two highly undesired side effects: It induces bleeding disorders and low blood pressure. de Oliveira et al. (2020) tested azithromycin, hydroxychloroquine and chloroquine by molecular dynamics against SARS-CoV-2 RBD. These drugs do bind to RBD, but with low energy.

Here, we employed an *in silico* approach but with a different idea, focused on SARS-CoV-2 spike protein, specifically in the RBD domain. Instead of looking for molecules to interact with the ACE2 receptor, we used the sequence of the human ACE2 receptor to design synthetic peptides derived from it to target S-RBD. Out of 259 peptides (Supplementary Tables S1–S3), ACE2-dev-pepI, ACE2-dev-pepII, ACE2-dev-pepIII and ACE2-dev-pepIV deserved attention.

Molecular docking and dynamic simulations revealed that all ACE2-derived peptides interacted efficiently with S-RBD (Table 1, Figures 1–8). This is a pioneer study employing quantum biochemistry to analyze peptides' interaction against SARS-CoV-2 RBD (Supplementary Tables S4–S7). Quantum biochemistry calculations (Morais et al., 2020) revealed the individual contribution of each amino acid residue of the ACE2-derived peptides and those of S-RBD. Therefore, these analyses showed that hydrogen bonds and ionic, aromatic, cation–pi and hydrophobic interactions are essential to attractive or repulsive interactions between the ACE2-derived peptides and S-RBD (Figures 3–7). As shown in Figure 8, the quantum biochemical calculations taking into consideration each amino acid energy level showed that the total interaction energy values between SARS-CoV-2 RBD and ACE2-dev-pepI, ACE2-dev-pepII, ACE2-dev-pepIII and ACE2-dev-pepIV were −64.9, −112.8, −84.6 and 1139 kcal.mol^{-1}, respectively (Figure 8). Further based on the quantum calculations, ACE2-dev-pepIV was the peptides with the highest

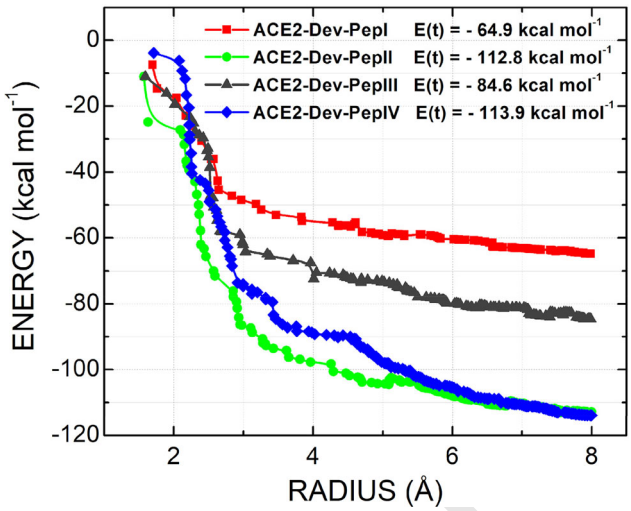

COLOR Online / B&W in Print

Figure 8. Total interaction energy between SARS-CoV-2 RBD and the ACE2-derived peptides as a function of the interaction distance. Red, green, black and blue squares represent ACE2-Dev-PepI, ACE2-Dev-PepII, ACE2-Dev-PepIII and ACE2-Dev-PepIV, respectively. E(t) is the sum of the interaction energies up to 8 Å.

affinity to bind with S-RBD, followed by ACE2-dev-pepII, ACE2-dev-pepIII and ACE2-dev-pepI.

Since this is the first study to apply quantum biochemistry calculations to analyze the interactions of peptides with S-RBD, our results can only be compared with those reported by Campos et al. (2020), who also investigated the interaction of two peptides against the Zika virus protease. By quantum biochemistry, the authors showed that the interaction energies of the peptides cn-716 and acyl-KR-aldehyde with the protease NS2B–NS3 were −63.35 kcal.mol^{-1} and −71.4 kcal.mol^{-1}, respectively. Our peptides interacted with S-RBD even more strongly than did cn-716 and acyl-KR-aldehyde to the protease NS2B–NS3.

Moreover, the effectiveness of other non-peptide-like antiviral drugs against S-RBD has been assayed. For example, de Oliveira et al. (2020) tested by molecular docking the interaction of the drugs azithromycin, hydroxychloroquine and chloroquine, which are used to treat bacterial infection and malaria, respectively, and study is about drug repositioning or repurposing, employed to speed up the drug discovery process by identifying a novel clinical use for an existing drug approved for a different indication (Yan et al., 2020). Our results revealed that ACE-derived peptides strongly bind to S-RBD. However, two questions remain; what are the consequences of that interaction? Can these peptides block or induce a wrong interaction between S-RBD and ACE2? The results presented here guide us to answer yes. As presented in Figure 9, the crystal structure (Figure 9(A)), the redocking of those structures (Figure 9(B)), and all ACE2-derived peptides when complexed with S-RBD did not block interaction between S-RBD and the ACE2 receptor, instead inducing an incorrect interaction between them (Figure (C–F)). These results strongly suggest that ACE2-derived peptides are efficient to prevent SARS-CoV-2 entry in cells, greatly reducing SARS-CoV-2 replication and avoiding COVID-19 establishment.

As expected, the ACE2-derived peptides presented high affinity to bind with S-RBD, and the results suggest these

COLOR Online / B&W in Print

Figure 9. The ACE2-derived peptides induced an abnormal interaction between SARS-CoV-2 RBD and the human ACE2 protein. Redocking (B) confirmed the accuracy of the molecular docking method used, with no difference for the crystallized structure (A). When SARS-CoV-2 RBD interacted with ACE2-Dev-PepI (C), ACE2-Dev-PepII (D), ACE2-Dev-PepIII (E) and ACE2-Dev-PepIV (F), the peptides could not interact correctly with human ACE2.

peptides are efficient to block SARS-CoV-2 infection. Additionally, for being designed from a human protein, these peptides will likely cause no serious collateral effects, unlike other drugs. The *in silico* analyses revealed these peptides have no toxic, allergenic or hemolytic potential against humans. Additionally, stability tests suggested high stability of ACE2-Dev-pepI, ACE2-Dev-pepII and ACE2-Dev-pepIV in the intestinal environment indicating possible oral administration.

5. Conclusion

Quantum biochemistry and molecular dynamic simulations revealed that the ACE2-derived peptides interact physically with S-RBD, blocking its interaction with the ACE2 receptor and thus virus entry in the cell. These findings suggest that ACE2-derived peptides are small antiviral molecules that can potentially prevent cell invasion by SARS-CoV-2 and thus its

replication *in vivo*. However, further investigation is required to prove this hypothesis. In conclusion, this pioneering *in silico* investigation opens an opportunity for further *in vivo* investigations of these peptides, aiming to discover new drugs and entirely new perspectives to treat COVID-19. For instance, peptide-based therapeutics have various advantages compared to traditional small-molecule drugs, such as higher specificity to selected targets, low toxicity because accumulation in the body is improbable, and less complex, costly and time-consuming synthesis (Yan et al., 2020).

Disclosure statement

No potential conflict of interest was reported by the authors.

Funding

Q4 Grants from the following Brazilian agencies supported this work: The National Council for Scientific and Technological Development (CNPq), with a doctoral grant to JLA and a research grant (codes 431511/2016-0 and 306202/2017-4) to JTAO; the Office to Coordinate Improvement of University Personnel (CAPES) sponsored PFNS with a postdoctoral fellowship. The authors are also grateful for the support received from the National Center for High-Performance Processing – Federal University of Ceará and Center for Ongoing Education in Health Care-CEATS/School of Public Health of Ceará (ESP-CE).

ORCID

Pedro F. N. Souza http://orcid.org/0000-0003-2524-4434

References

Amaral, J. L., Santos, S. J. M., Souza, P. F. N., de Morais, P. A., Maia, F. F., Carvalho, H. F., & Freire, V. N. (2020). Quantum biochemistry in cancer immunotherapy: New insights about CTLA-4/ipilimumab and design of ipilimumab-derived peptides with high potential in cancer treatment. *Molecular Immunology*, *127*, 203–211. https://doi.org/10.1016/j.molimm.2020.09.013

Q5

Andersen, K. G., Rambaut, A., Lipkin, W. I., Holmes, E. C., & Garry, R. F. (2020). The proximal origin of SARS-CoV-2. *Nature Medicine*, *26*(4), 450–452. https://doi.org/10.1038/s41591-020-0820-9

Burrell, C. J., Howard, C. R., & Murphy, F. A. (2017). Chapter 13 – Coronaviruses. In *Fenner and White's Medical Virology* (5th ed., pp. 437–446). https://doi.org/10.1016/B978-0-12-375156-0.00031-X.

Q6

Calligari, P., Bobone, S., Ricci, G., & Bocedi, A. (2020). Molecular investigation of SARS–CoV-2 proteins and their interactions with antiviral drugs. *Viruses*, *12*(4), 445–460. https://doi.org/10.3390/v12040445

Campos, D. M. O., Bezerra, K. S., Esmaile, S. C., Fulco, U. L., Albuquerque, E. L., & Oliveira, J. I. N. (2020). Intermolecular interactions of cn-716 and acyl-KR-aldehyde dipeptide inhibitors against Zika virus. *Physical Chemistry Chemical Physics: PCCP*, *22*(27), 15683–15695. https://doi.org/10.1039/d0cp02254c

Choudhary, S., Malik, Y. S., & Tomar, S. (2020). Identification of SARS-CoV-2 cell entry inhibitors by drug repurposing using in silico structure-based virtual screening approach. *Frontiers in Immunology*, *11*, 1664. https://doi.org/10.3389/fimmu.2020.01664

de Oliveira, O. V., Rocha, G. B., Paluch, A. S., & Costa, L. T. (2020). Repurposing approved drugs as inhibitors of SARS-CoV-2 S-protein from molecular modeling and virtual screening. *Journal of Biomolecular Structure and Dynamics*, 1–10. https://doi.org/10.1080/07391102.2020.1772885.

Q7

Delley, B. (2000). From molecules to solids with the DMol3 approach. *Journal of Chemical Physics*, *113*(18), 7756–7764. https://doi.org/10.1063/1.1316015

Diamond, M. S., & Pierson, T. C. (2020). The challenges of vaccine development against a new virus during a pandemic. *Cell Host & Microbe*, *27*(5), 699–703. https://doi.org/10.1016/j.chom.2020.04.021

Elfiky, A. A. (2020). Ribavirin, Remdesivir, Sofosbuvir, Galidesivir, and Tenofovir against SARS-CoV-2 RNA dependent RNA polymerase (RdRp): A molecular docking study. *Life Sciences*, *253*, 117592. https://doi.org/10.1016/j.lfs.2020.117592

Hall, D. C., & Ji, H.-F. (2020). A search for medications to treat COVID-19 via in silico molecular docking models of the SARS-CoV-2 spike glycoprotein and 3CL protease. *Travel Medicine and Infectious Disease*, *35*, 101646. https://doi.org/10.1016/j.tmaid.2020.101646

Henderson, R., Edwards, R. J., Mansouri, K., Janowska, K., Stalls, V., Gobeil, S. M. C., Kopp, M., Li, D., Parks, R., Hsu, A. L., Borgnia, M. J., Haynes, B. F., & Acharya, P. (2020). Controlling the SARS-CoV-2 spike glycoprotein conformation. *Nature Structural & Molecular Biology*. https://doi.org/10.1038/s41594-020-0479-4.

Q8

Hoffmann, M., Kleine-Weber, H., Schroeder, S., Krüger, N., Herrler, T., Erichsen, S., Schiergens, T. S., Herrler, G., Wu, N. H., Nitsche, A., Müller, M. A., Drosten, C., & Pöhlmann, S. (2020). SARS-CoV-2 cell entry depends on ACE2 and TMPRSS2 and is blocked by a clinically proven protease inhibitor. *Cell*, *181*(2), 271–280.e8. https://doi.org/10.1016/j.cell.2020.02.052

Korber, B., Fischer, W. M., Gnanakaran, S., Yoon, H., Theiler, J., Abfalterer, W., Hengartner, N., Giorgi, E. E., Bhattacharya, T., Foley, B., Hastie, K. M., Parker, M. D., Partridge, D. G., Evans, C. M., Freeman, T. M., de Silva, T. I., McDanal, C., Perez, L. G., Tang, H., … Montefiori, D. C, Sheffield COVID-19 Genomics Group (2020). Tracking changes in SARS-CoV-2 spike: Evidence that D614G increases infectivity of the COVID-19 virus. *Cell*, *182*(4), 812–827. https://doi.org/10.1016/j.cell.2020.06.043

Laskowski, R. A., & Swindells, M. B. (2011). LigPlot+: Multiple ligand-protein interaction diagrams for drug discovery. *Journal of Chemical Information and Modeling*, *51*(10), 2778–2786. https://doi.org/10.1021/ci200227u

Li, H., Liu, L., Zhang, D., Xu, J., Dai, H., Tang, N., Su, X., & Cao, B. (2020). SARS-CoV-2 and viral sepsis: Observations and hypotheses. *Lancet (London, England)*, *395*(10235), 1517–1520. https://doi.org/10.1016/S0140-6736(20)30920-X

Li, Q., Guan, X., Wu, P., Wang, X., Zhou, L., Tong, Y., Ren, R., Leung, K. S. M., Lau, E. H. Y., Wong, J. Y., Xing, X., Xiang, N., Wu, Y., Li, C., Chen, Q., Li, D., Liu, T., Zhao, J., Liu, M. … Feng, Z. (2020). Early transmission dynamics in Wuhan, China, of novel coronavirus-infected pneumonia. *The New England Journal of Medicine*, *382*(13), 1199–1207. https://doi.org/10.1056/NEJMoa2001316

Meher, P. K., Sahu, T. K., & Rao, A. R. (2016). Prediction of donor splice sites using random forest with a new sequence encoding approach. *BioData Mining*, *9*, 4. https://doi.org/10.1186/s13040-016-0086-4

Moal, I. H., & Bates, P. A. (2010). SwarmDock and the use of normal modes in protein-protein docking. *International Journal of Molecular Sciences*, *11*(10), 3623–3648. https://doi.org/10.3390/ijms11103623

Morais, P. A., Maia, F. F., Solis-Calero, C., Caetano, E. W. S., Freire, V. N., & Carvalho, H. F. (2020). The urokinase plasminogen activator binding to its receptor: A quantum biochemistry description within an in/homogeneous dielectric function framework with application to uPA-uPAR peptide inhibitors. *Physical Chemistry Chemical Physics*, *22*(6), 3570–3583. https://doi.org/10.1039/C9CP06530J

Moreira, R. A., Chwastyk, M., Baker, J. L., Guzman, H. V., & Poma, A. B. (2020). Quantitative determination of mechanical stability in the novel coronavirus spike protein. *Nanoscale*, *12*(31), 16409–16413. https://doi.org/10.1039/d0nr03969a

Ngo, S. T., Quynh Anh Pham, N., Thi Le, L., Pham, D.-H., & Vu, V. V. (2020). Computational determination of potential inhibitors of SARS-CoV-2 main protease. *Journal of Chemical Information and Modeling*, *60*(12), 5771–5780. https://doi.org/10.1021/acs.jcim.0c00491

Othman, H., Bouslama, Z., Brandenburg, J.-T., da Rocha, J., Hamdi, Y., Ghedira, K., Srairi-Abid, N., & Hazelhurst, S. (2020). Interaction of the spike protein RBD from SARS-CoV-2 with ACE2: Similarity with SARS-CoV, hot-spot analysis and effect of the receptor polymorphism.

Biochemical and Biophysical Research Communications, *527*(3), 702–708. https://doi.org/10.1016/j.bbrc.2020.05.028

Peiris, J. S. M. (2012). Coronaviruses. In *Medical Microbiology* (pp. 587–593). Elsevier. https://doi.org/10.1016/B978-0-7020-4089-4.00072-X.

Qiao, B., & Olvera de la Cruz, M. (2020). Enhanced binding of SARS-CoV-2 spike protein to receptor by distal polybasic cleavage sites. *ACS Nano*, *14*(8), 10616–10623. https://doi.org/10.1021/acsnano.0c04798

Ramírez-Aportela, E., López-Blanco, J. R., & Chacón, P. (2016). FRODOCK 2.0: Fast protein-protein docking server. *Bioinformatics (Oxford, England)*, *32*(15), 2386–2388. https://doi.org/10.1093/bioinformatics/btw141

Robertson, M. J., Tirado-Rives, J., & Jorgensen, W. L. (2015). Improved peptide and protein torsional energetics with the OPLSAA force field. *Journal of Chemical Theory and Computation*, *11*(7), 3499–3509. https://doi.org/10.1021/acs.jctc.5b00356

Shen, Y., Maupetit, J., Derreumaux, P., & Tufféry, P. (2014). Improved PEP-FOLD approach for peptide and miniprotein structure prediction. *Journal of Chemical Theory and Computation*, *10*(10), 4745–4758. https://doi.org/10.1021/ct500592m

Song, Z., Xu, Y., Bao, L., Zhang, L., Yu, P., Qu, Y., Zhu, H., Zhao, W., Han, Y., & Qin, C. (2019). From SARS to MERS, thrusting coronaviruses into the spotlight. *Viruses*, *11*(1), 59. https://doi.org/10.3390/v11010059

Souza, P. F. N., Lopes, F. E. S., Amaral, J. L., Freitas, C. D. T., & Oliveira, J. T. A. (2020). A molecular docking study revealed that synthetic peptides induced conformational changes in the structure of SARS-CoV-2 spike glycoprotein, disrupting the interaction with human ACE2 receptor. *International Journal of Biological Macromolecules*, *164*, 66–76. https://doi.org/10.1016/j.ijbiomac.2020.07.174

Souza, P. F. N., Marques, L. S. M., Oliveira, J. T. A., Lima, P. G., Dias, L. P., Neto, N. A. S., Lopes, F. E. S., Sousa, J. S., Silva, A. F. B., Caneiro, R. F., Lopes, J. L. S., Ramos, M. V., & Freitas, C. D. T. (2020). Synthetic antimicrobial peptides: From choice of the best sequences to action mechanisms. *Biochimie*, *175*, 132–145. https://doi.org/10.1016/j.biochi.2020.05.016

Tay, M. Z., Poh, C. M., Rénia, L., MacAry, P. A., & Ng, L. F. P. (2020). The trinity of COVID-19: Immunity, inflammation and intervention. *Nature Reviews Immunology*, *20*(6), 363–374. https://doi.org/10.1038/s41577-020-0311-8

Thakur, N., Qureshi, A., & Kumar, M. (2012). AVPpred: Collection and prediction of highly effective antiviral peptides. *Nucleic Acids Research*, *40*(Web Server issue), W199–W204. https://doi.org/10.1093/nar/gks450

Walls, A. C., Park, Y.-J., Tortorici, M. A., Wall, A., McGuire, A. T., & Veesler, D. (2020). Structure, function, and antigenicity of the SARS-CoV-2 spike glycoprotein. *Cell*, *181*(2), 281–292.e6. https://doi.org/10.1016/j.cell.2020.02.058

Wrapp, D., Wang, N., Corbett, K. S., Goldsmith, J. A., Hsieh, C. L., Abiona, O., Graham, B. S., & McLellan, J. S. (2020). Cryo-EM structure of the 2019-nCoV spike in the prefusion conformation. *Science (New York, NY)*, *367*(6483), 1260–1263. https://doi.org/10.1126/science.abb2507

Wu, C., Liu, Y., Yang, Y., Zhang, P., Zhong, W., Wang, Y., Wang, Q., Xu, Y., Li, M., Li, X., Zheng, M., Chen, L., & Li, H. (2020). Analysis of therapeutic targets for SARS-CoV-2 and discovery of potential drugs by computational methods. *Acta Pharmaceutica Sinica. B*, *10*(5), 766–788. https://doi.org/10.1016/j.apsb.2020.02.008

Yan, R., Zhang, Y., Li, Y., Xia, L., Guo, Y., & Zhou, Q. (2020). Structural basis for the recognition of SARS-CoV-2 by full-length human ACE2. *Science (New York, NY)*, *367*(6485), 1444–1448. https://doi.org/10.1126/science.abb2762

Yuan, Y., Cao, D., Zhang, Y., Ma, J., Qi, J., Wang, Q., Lu, G., Wu, Y., Yan, J., Shi, Y., Zhang, X., & Gao, G. F. (2017). Cryo-EM structures of MERS-CoV and SARS-CoV spike glycoproteins reveal the dynamic receptor binding domains. *Nature Communications*, *8*, 15092. https://doi.org/10.1038/ncomms15092

Zhang, Y., Xu, J., Jia, R., Yi, C., Gu, W., Liu, P., Dong, X., Zhou, H., Shang, B., Cheng, S., Sun, X., Ye, J., Li, X., Zhang, J., Ling, Z., Ma, L., Wu, B., Zeng, M., Zhou, W., & Sun, B. (2020). Protective humoral immunity in SARS-CoV-2 infected pediatric patients. *Cellular & Molecular Immunology*, *17*(7), 768–770. https://doi.org/10.1038/s41423-020-0438-3

Zhang, D. W., & Zhang, J. Z. H. (2003). Molecular fractionation with conjugate caps for full quantum mechanical calculation of protein-molecule interaction energy. *Journal of Chemical Physics*, *119*(7), 3599–3605. https://doi.org/10.1063/1.1591727

Zhou, P., Yang, X. L., Wang, X. G., Hu, B., Zhang, L., Zhang, W., Si, H. R., Zhu, Y., Li, B., Huang, C. L., Chen, H. D., Chen, J., Luo, Y., Guo, H., Jiang, R. D., Liu, M. Q., Chen, Y., Shen, X. R., Wang, X. … Shi, Z.-L. (2020). A pneumonia outbreak associated with a new coronavirus of probable bat origin. *Nature*, *579*(7798), 270–273. https://doi.org/10.1038/s41586-020-2012-7